Cancer Cell International

RESEARCH

Open Access

Does rAj-Tspin, a novel peptide from *A. japonicus*, exert antihepatocellular carcinoma effects via the ITGB1/ZYX/FAK/AKT signaling pathway?

Ying Che[1†], Xiaolong Lu[1†], Xueting Wang[1], Zhien Liu[1], Liyang Guan[1], Xin Li[1], Zaixing Du[1], Hang Ren[1], Jihong Wang[3*], Zunchun Zhou[2*] and Li Lv[1*]

Abstract

rAj-Tspin, a soluble recombinant peptide from *Apostichopus japonicus*, can inhibit the integrin β1 (ITGB1)/FAK/AKT signaling pathway in hepatocellular carcinoma (HCC) via cell epithelial–mesenchymal transition (EMT) and apoptosis. Zyxin (ZYX) is a focal adhesion protein that is considered a novel mediator of EMT and apoptosis. However, the inhibitory mechanisms of rAj-Tspin in HCC and whether it is related to ZYX are unclear. We examined the antitumor effect of rAj-Tspin on the Huh7 human HCC cell line and on a nude mouse model generated via subcutaneous injection or orthotopic intrahepatic transplantation of Huh7 cells. Our results revealed that rAj-Tspin strikingly reduced the viability and promoted the apoptosis of Huh7 cells and inhibited HCC tumor growth in nude mice. rAj-Tspin inhibited ITGB1 and ZYX protein expression in vivo and in vitro in a dose-dependent manner. Mechanistically, the FAK/AKT signaling pathway and the proliferation and invasion of HCC cells were suppressed upon ITGB1 and ZYX knockdown. Moreover, the effect of ITGB1 overexpression on the growth of HCC cells was inhibited by rAj-Tspin. In contrast, the promoting effect of ITGB1 overexpression could be inhibited by ZYX knockdown. ZYX knockdown had no effect on ITGB1 expression. These findings suggest that ZYX is required for the indispensable role of ITGB1 in rAj-Tspin-alleviated HCC and provide an important therapeutic target for HCC. In summary, the anti-HCC effect of rAj-Tspin potentially involves the regulation of the ITGB1/ZYX/FAK/AKT pathway, which in turn impacts EMT and apoptosis.

Keywords Hepatocellular carcinoma, rAj-Tspin, ITGB1, ZYX, EMT, Apoptosis

[†]Ying Che and Xiaolong Lu contributed equally to this work.

*Correspondence:
Jihong Wang
jihongwang999@lnnu.edu.cn
Zunchun Zhou
zunchunz@hotmail.com
Li Lv
lv_li@126.com
Full list of author information is available at the end of the article

Graphical Abstract

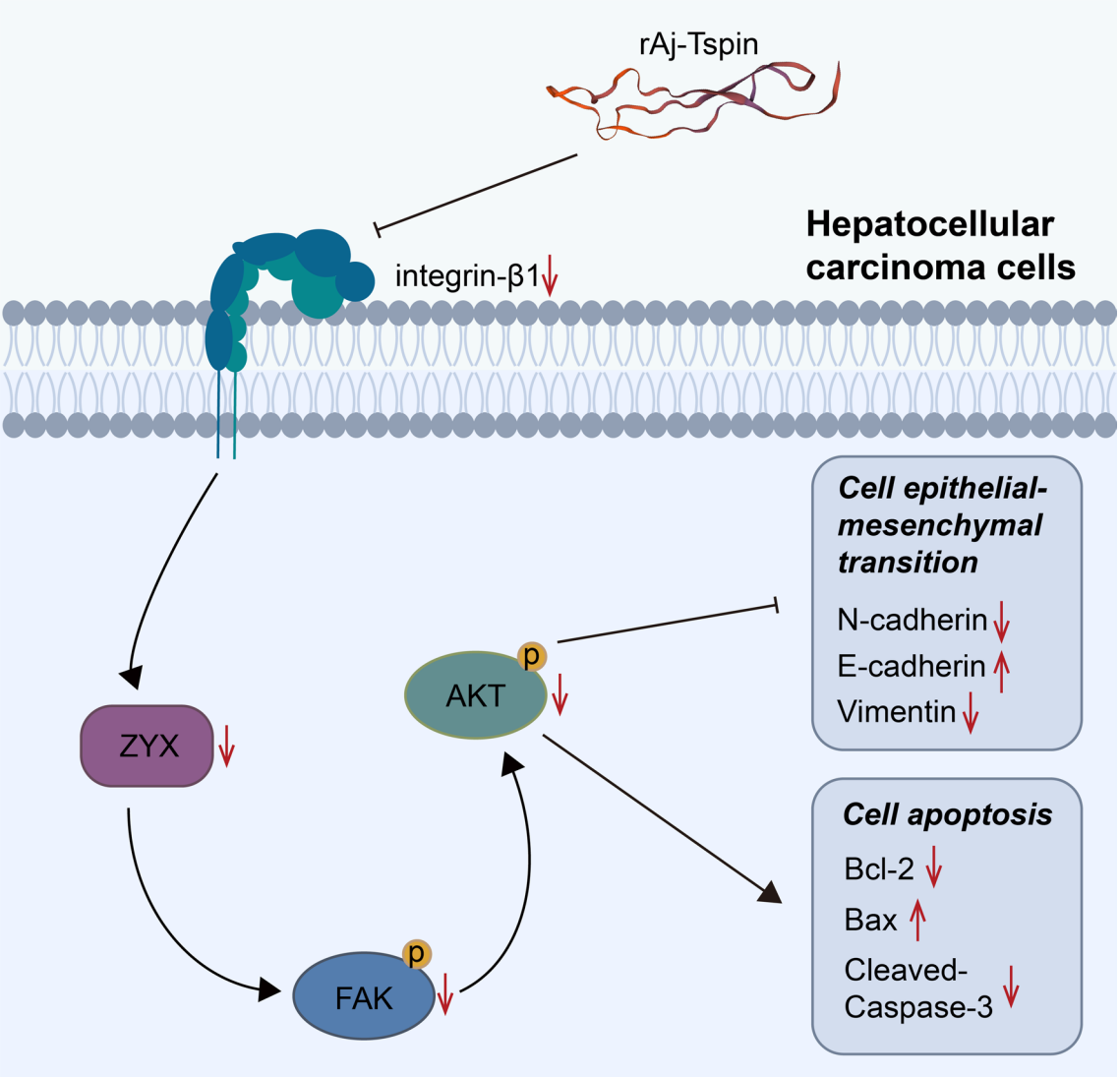

Introduction

Hepatocellular carcinoma (HCC) is the third leading cause of cancer-related mortality worldwide [1]. The increasing incidence and mortality of HCC pose considerable challenges to global healthcare. Patients with HCC have an unfavorable prognosis, and intrahepatic and extrahepatic metastases often occur because of their aggressive features [2]. The current treatment options for HCC are limited [3]. Recently, combination strategies involving the integration of systemic and locoregional therapies, such as transarterial chemoembolization (TACE) in conjunction with systemic therapy [4], neoadjuvant combination therapy [5], atezolizumab combined with Bevacizumab [6], and the other combination treatments based on immune checkpoint inhibitor (ICI) [7], have presented highly promising avenues for further investigation. Significant progress has been made in the treatment of HCC with the application of new first- and second-line agents; however, their efficacy is limited, and they are only effective for some patients or only prolong survival by several months [8]. As such, new therapeutic agents and targets are urgently needed to improve outcomes in patients with HCC.

rAj-Tspin is a soluble gene recombinant peptide from *Apostichopus japonicus* (*A. japonicus*). *A. japonicus* belongs to the phylum Echinoderm and has a variety of biological activities [9]. Bioinformatics analysis of *A. japonicus* sequences via cDNA libraries revealed a high abundance of "a disintegrin and metalloproteinase with thrombospondin motifs". Further analysis of the sequence via the ExPASy website revealed that it contains 10 thrombin-sensitive protein-1 (TSP-1) domains. The 168-bp cDNA sequence of the third TSP-1 domain in arginine-glycine-aspartic acid (RGD) mode was synthesized, cloned and expressed, and the 6975.53-Da recombinant peptide obtained via expression was named rAj-Tspin [10]. Growing evidence suggests that animal-derived RGD motile active peptides, namely, disintegrins, can competitively bind to integrin receptors, thereby blocking integrin-related signaling pathways, preventing the invasion and adhesion of tumor cells, and even promoting the apoptosis of tumor cells [11, 12]. We previously showed that rAj-Tspin contributes to ITGB1/FAK/AKT in BEL-7402 HCC cells. Therefore, rAj-Tspin undoubtedly has therapeutic potential in the clinical treatment of HCC [13].

The importance of EMT and apoptosis in cancer treatment has been highlighted by recent findings regarding the associations of EMT and apoptosis with tumor progression and drug response [14]. It has been suggested that zyxin (ZYX), a focal adhesion protein that regulates EMT and apoptosis, is involved in multiple cancers, including colon cancer, breast cancer, prostate cancer, and lung cancer [15–17]. However, the relevant mechanism and whether it participates in HCC are unclear. Focal adhesions (FAs) are cell–matrix contacts formed by a nascent adhesion complex composed of integrins and numerous other focal adhesion molecules, such as talin, paxillin, zyxin, VASP, and FAK [18]. In particular, ITGB1 is widely reported in hepatocellular carcinoma and plays an indispensable role in focal adhesion [19]. However, the molecular mechanism by which rAj-Tspin affects ZYX and ITGB1 to alleviate HCC remains unclear.

In the present study, we used the Huh7 human HCC cell line in vitro and constructed in vivo nude mouse models via the subcutaneous and orthotopic intrahepatic transplantation of Huh7 cells to investigate whether the inhibition of ZYX and ITGB1 by rAj-Tspin can inhibit EMT and apoptosis-mediated HCC by decreasing the phosphorylation level of FAK/AKT.

Materials and methods

Cell culture

The human HCC cell line Huh7 and the immortalized human liver cell line LO2 were maintained in high-glucose Dulbecco's modified Eagle's medium (DMEM, Gibco) supplemented with 10% fetal bovine serum (FBS, Gibco) and 1% penicillin–streptomycin (HyClone). All cells were donated by the College of Life Sciences at Liaoning Normal University (Dalian, China) and grown at 37 °C in a humidified atmosphere containing 5% CO_2.

Subcutaneous and orthotopic intrahepatic transplantation model

For generation of the subcutaneous transplantation model, 1×10^7 Huh7 cells were detached and suspended in 100 μL of serum-free DMEM/Matrigel (9:1). The cells were subcutaneously injected into BALB/c-nude mice (male, 5 weeks old, n = 8 per group) [20]. For generation of the orthotopic intrahepatic transplantation model, 1×10^6 Huh7 cells in 20 μL of serum-free DMEM were injected into each BALB/c-nude mouse. Through a 1 cm transverse incision in the upper abdomen under anesthesia, the cells were injected into the left hepatic lobe of each mouse (male, 5 weeks old, n = 6 per group) [21]. The mice were randomly divided into the saline group, rAj-Tspin (50 μg/kg) group, rAj-Tspin (100 μg/kg) group and rAj-Tspin (200 μg/kg) group, and the treatments were administered i.p. twice daily. The body weights of the nude mice and the larger diameter of the tumor a (mm) and the smaller diameter b (mm) were measured and recorded every other day, and the tumor volume was calculated as $V = a\times b^2/2$. All the mice were sacrificed after 2 weeks, and the tumors and livers were collected, fixed with neutral formalin and prepared for histological examination. All the mice were treated and housed according to the methods of the Feeding and Management of Experimental Animals of Dalian Medical University.

Histopathological staining

The liver tissues of the mice were embedded in paraffin to produce 5-μm-thick sections. The tissue slices were stained with hematoxylin and eosin (H&E) to observe the tissue structure. An optical microscope (OLYMPUS) was used to detect pathological changes and target protein expression in each tissue section.

Cell viability assay

Huh7 cells were seeded on 96-well plates (5×10^3 cells/well) for 12–16 h and then treated with rAj-Tspin at various concentrations for 24 h, 48 h, or 72 h. The cells were further incubated with 10% CCK-8 solution (Bioss) at 37 °C for 2 h, after which the absorbance at 450 nm was measured via a microplate reader (TECAN).

Small interfering RNA and plasmid transfection

Transfection with ZYX/ITGB1 small interfering RNA (siRNA; GenePharma) and an ITGB1-overexpressing plasmid (GenePharma) was performed via Mate (GenePharma)

according to the standardized protocol. ZYX siRNA: 5′-GUGUUACAAGUGUGAGGACTT-3′; ITGB1 siRNA: 5′-GCGAGTGTGATAATTTCAA-3′. siRNA was used to suppress ZYX/ITGB1 expression in Huh7 cells, and a recombinant plasmid construct of the gene was used to overexpress ITGB1 in Huh7 cells.

Cell migration assay

Huh7 cells were seeded on 6-well plates (2×10^5 cells/well) for 24 h, wounded by scratching with sterile plastic 200-μL micropipette tips, and photographed via an inverted microscope (GROUPCR). After treatment with rAj-Tspin (0, 0.2, 0.4 or 0.8 μM) for 24 h or transfection, the culture wells were photographed again.

Cell invasion assay

Transwell chambers (Costar) were precoated with 50 μL of serum-free DMEM/Matrigel (9:1) to facilitate the assessment of cell migration. Pretreated Huh7 cells (1×10^4) in 200 μL of serum-free medium were plated in the upper chamber, and 700 μL of culture medium supplemented with 10% FBS was added to the lower chamber. After a 24-h incubation, the migrated cells were fixed with 4% paraformaldehyde (Servicebio) and stained with 0.3% crystal violet (Solarbio). Three fields were selected at random through photography, and their numbers were documented.

Cell adhesion assay

For this assay, 96-well plates were precoated with 50 μL of 10 μg/mL fibronectin (FN, Solarbio) and sealed with 1% bovine serum albumin (BSA, Solarbio) at 37 °C for 1 h to facilitate the assessment of cell adhesion. Pretreated Huh7 cells (5×10^3) in 100 μL were seeded in 96-well plates. After a 2-h incubation, the cells were fixed and stained with 0.3% crystal violet. Three fields were selected at random and photographed. The dye was extracted with 33% acetic acid, and the absorbance at 600 nm was detected with a microplate reader.

TUNEL assay

Huh7 cells were seeded on 24-well plates (1×10^4 cells/well) for 24 h and then treated with rAj-Tspin (0, 0.2, 0.4 or 0.8 μM) for 24 h or transfected. After fixation with 4% paraformaldehyde and permeabilization with 0.3% Triton X-100 (Solarbio), the cells were incubated with TUNEL solution (Beyotime) for 2 h in the dark. The nuclei were stained with DAPI (Solarbio), and three fields were selected at random through photography.

Western blotting

Total protein was extracted from tissues or cells via RIPA buffer (Beyotime) containing PMSF (Beyotime). The lysate was then sonicated and centrifuged at 4 °C at 12,000 r/min for 10 min. The samples were added to 2×loading buffer, followed by a denaturation step at 100 °C. All proteins were subjected to 8–12% sodium dodecyl sulfate–polyacrylamide gel electrophoresis (SDS-PAGE; concentrated gel, 80 V; separator gel, 120 V) and transferred to PVDF membranes (Millipore). Afterward, the membrane was blocked with 10% skim milk at room temperature for 2 h and incubated overnight at 4 °C with primary antibodies against the following targets: ITGB1 (ab183666, Abcam), FAK (3285 s, CST), p-FAK (3283 s, CST), AKT (10176-2-AP, Proteintech), p-AKT (28731-1-AP, Proteintech), ZYX (10330-1-AP, Proteintech), N-cadherin (22018-1-AP, Proteintech), E-cadherin (20874-1-AP, Proteintech), vimentin (10366-1-AP, Proteintech), Bax (60267-1-Ig, Proteintech), Bcl-2 (12789-1-AP, Proteintech), cleaved caspase-3 (abs132005, Absin), and GAPDH (10494-1-AP, Proteintech). After several washes, the membrane was incubated with anti-mouse IgG or anti-rabbit IgG for 2 h and detected using ECL reagent (Meilunbio) and an imaging system (Tanon). The blots were quantified via ImageJ software.

Coimmunoprecipitation (Co-IP) assay

Total protein was extracted from cells via lysis buffer. The relevant antibodies and protein A/G beads were added to the protein lysates. Afterward, the lysates were incubated at 4 °C overnight. The samples were then subjected to SDS–PAGE electrophoresis by adding 1×loading buffer followed by a denaturation step at 100 °C.

Immunofluorescence

Huh7 cells were seeded on 24-well plates (1×10^4 cells/well) at a confluence of 60%–80%. After fixation and permeabilization, the cells were incubated with primary antibodies at 4 °C overnight, labeled with secondary antibodies and counterstained with DAPI. Images were acquired via reverse fluorescence microscopy.

Bioinformatics analysis

Gene Expression Profiling Interactive Analysis (GEPIA, URL: http://gepia.cancer-pku.cn) was conducted to analyze the expression of ZYX in HCC tumor tissue and normal tissue. The University of Alabama at Birmingham (UALCAN, URL: http://ualcan.path.uab.edu) conducted an online analysis of Kaplan–Meier plots related to the ZYX gene in HCC patients.

Statistical analysis

Data analysis was performed via SPSS 22.0 software. All the data are expressed as the means ± standard deviations (SDs). The two groups of data were compared via the independent sample *t* test, and comparisons of multiple

variables were performed via one-way analysis of variance. Statistical analysis was performed via the use of GraphPad Prism 8.4.3 software to draw column graphs. Statistical significance was defined as $P < 0.05$.

Results

rAj-Tspin inhibited the growth of subcutaneous tumors and orthotopic intrahepatic tumors derived from Huh7 cells

To evaluate the effectiveness of rAj-Tspin on HCC growth in vivo, we subcutaneously and intrahepatically inoculated Huh7 cells into nude mice (Fig. 1A). We observed that the administration of rAj-Tspin resulted in a dose-dependent reduction in both the volume and weight of xenograft tumors but had no effect on the body weight of the mice (Fig. 1B–E). In addition, we performed HE staining on the xenograft tumors, further demonstrating the antitumor effect of rAj-Tspin in vivo (Fig. 1F). In the orthotopic intrahepatic transplantation model, we observed a dose-dependent reduction in the tumor area and in the size and number of nodules upon administration of rAj-Tspin (Fig. 1G). This finding was further confirmed by H&E staining. Furthermore, the rAj-Tspin-treated group presented significantly decreased serum LDH levels without affecting mouse body weight (Fig. 1H, I).

rAj-Tspin targeted ITGB1 and inhibited the high expression of ZYX and ITGB1 in vivo

rAj-Tspin has a strong affinity for the ITGB1 domain, and the potential binding sites are predicted to be residues Arg43, Arg48, and Cys55 (Fig. 2A). GEPIA revealed ZYX overexpression in HCC patient samples compared with normal samples (Fig. 2B, $P < 1e{-}12$). We investigated the association between high ZYX expression and patient survival by using UALCAN and found a significant correlation with poor prognosis (Fig. 2C, $P = 0.002$). Western blotting revealed higher ZYX and ITGB1 expression in liver cancer tissue than in normal tissue (Fig. 2D). Furthermore, rAj-Tspin attenuated the expression of ITGB1 and ZYX as well as the phosphorylation of FAK and AKT in vivo (Fig. 2E, F) in a dose-dependent manner.

rAj-Tspin repressed the growth of Huh7 cells in vitro

To evaluate the impact of rAj-Tspin on Huh7 cells, we exposed them to varying concentrations of rAj-Tspin for 24, 48, and 72 h via the CCK-8 assay. We observed a reduction in cell viability that was dependent on the dosage administered (Fig. 3A). The results of the cell scratch, Transwell and adhesion assays revealed that as the rAj-Tspin concentration increased, the migration, invasion and adhesion of Huh7 cells decreased (Fig. 3B). TUNEL assays indicated that rAj-Tspin promoted apoptosis in Huh7 cells in a dose-dependent manner (Fig. 3C). Western blot analysis revealed that the expression levels of ZYX and ITGB1 were greater in Huh7 cells than in LO2 cells (Fig. 3D). Similarly, the administration of rAj-Tspin resulted in a dose-dependent reduction in the expression levels of ITGB1 and ZYX as well as the phosphorylation levels of FAK and AKT in vitro (Fig. 3E). To further investigate the effects of rAj-Tspin on HCC apoptosis and EMT, we conducted Western blot analysis of apoptosis- and EMT-related proteins. The results revealed that cleaved caspase-3 and Bax levels were increased, the Bcl-2 level was decreased, the N-cadherin and vimentin levels were decreased, and the E-cadherin level was increased in HCC cells treated with rAj-Tspin (Fig. 3F). Thus, rAj-Tspin induced apoptosis and inhibited EMT in Huh7 cells. Collectively, these findings suggest that rAj-Tspin represses the growth of Huh7 cells through EMT and apoptosis in vitro.

Knockdown of ITGB1 suppressed Huh7 cell progression in vitro

To explore the potential biological function of ITGB1, we transfected Huh7 cells with ITGB1 siRNA. The migration, invasion and adhesion capacities (Fig. 4A) were significantly reduced in Huh7 cells transfected with si-ITGB1. The TUNEL assay results indicated that ITGB1 knockdown promoted apoptosis in Huh7 cells (Fig. 4B). Western blot assays revealed that silencing ITGB1 suppressed the expression of ZYX and the phosphorylation of FAK and AKT (Fig. 4C). Moreover, ITGB1 knockdown influenced the expression of apoptosis- and EMT-related proteins (Fig. 4D), inhibited EMT and induced apoptosis in Huh7 cells. These results indicate that ITGB1 plays an important role in suppressing features related to disease progression in HCC cells in vitro.

rAj-Tspin suppressed cell growth through ITGB1 inhibition in HCC cells

To further clarify the mechanism underlying whether ITGB1 is a potential trigger in rAj-Tspin-mediated suppression of cell growth, we established ITGB1-overexpressing cells. The overexpression of ITGB1 increased the proliferation, migration and adhesion ability of Huh7 cells, whereas rAj-Tspin intervention attenuated these effects (Fig. 5A). As expected, Western blot assays revealed that the overexpression of ITGB1 induced the accumulation of ZYX, increased the phosphorylation of FAK and AKT, and was effectively abolished by rAj-Tspin (Fig. 5B). Moreover, overexpression of ITGB1 suppressed apoptosis and triggered EMT in Huh7 cells, which was counteracted by rAj-Tspin treatment (Fig. 5C). In summary, these results demonstrate that the downregulation of ITGB1 is required for the rAj-Tspin-mediated suppression of HCC growth.

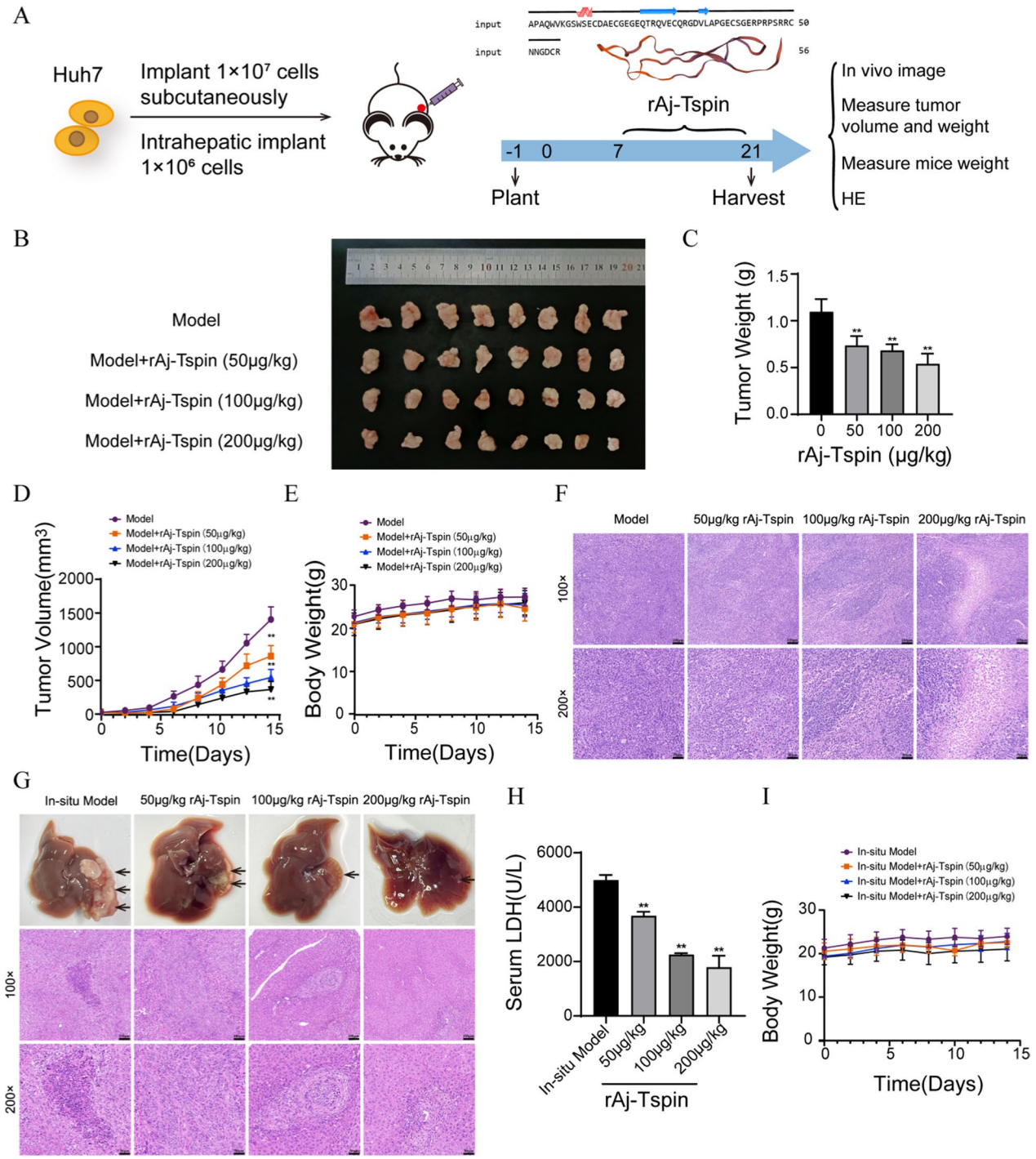

Fig. 1 Effects of rAj-Tspin inhibition on Huh7 subcutaneous grafts and an orthotopic intrahepatic transplantation model in nude mice. **A** Schematic diagram of xenografts in BALB/c nude mice generated via the inoculation of Huh7 cells at their underarm and intrahepatically, respectively. Then, the xenografts were treated with rAj-Tspin starting on the 7th day after injection, and the mice were sacrificed on the 21st day after injection. **B** Images (**C**) and weights of excised tumors from the control and rAj-Tspin (50, 100, and 200 μg/kg) groups of nude mice, **D** volumes measured at the indicated time points, **E** and effects of rAj-Tspin on body weight. **F** H&E staining of excised tumors from nude mice; scale bar = 100 μm (100×) and 50 μm (200×), n = 8. $^{**}P < 0.01$. **G** Representative images and H&E staining of liver tissues from mice orthotopically inoculated with Huh7 cells; scale bar = 100 μm (100×) and 50 μm (200×). **H** The release of serum LDH in nude mice was measured by LDH assay. (**I**) Effects of rAj-Tspin on the body weight of nude mice (n = 6). $^{**}P < 0.01$

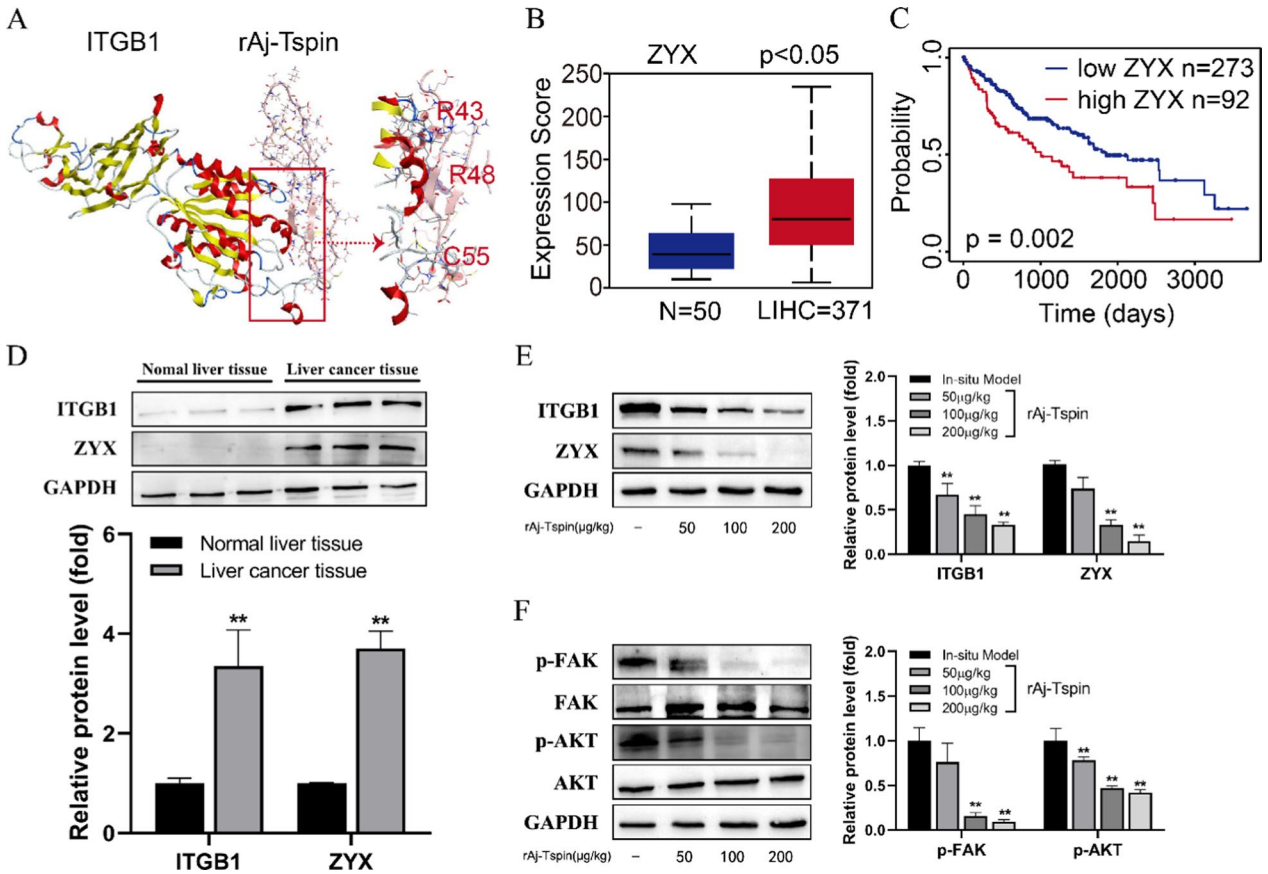

Fig. 2 rAj-Tspin targets ITGB1 to inhibit ITGB1/ZYX overexpression in HCC. **A** The chemical structure of rAj-Tspin and the docking conformation revealed the interaction of rAj-Tspin with the active site of ITGB1 via MOE software. **B** Expression of ZYX in normal tissues and liver cancer tissues in the GEPIA database. **C** Relationship between ZYX expression and the survival time of HCC patients in the UALCAN cancer database. **D** Immunoblotting of ITGB1 and ZYX in liver tissue. **E** and **F** Immunoblotting of ITGB1, ZYX, p-FAK, FAK, p-AKT, and AKT in liver tissue after rAj-Tspin treatment (n = 3). $^{**}P < 0.01$

Knockdown of ZYX suppressed Huh7 cell progression in vitro

To explore the specific role of ZYX in HCC cells, we transfected Huh7 cells with ZYX siRNA. The migration, invasion and adhesion capacities (Fig. 6A) were significantly reduced in Huh7 cells transfected with si-ZYX. The TUNEL assay results indicated that ZYX knockdown promoted apoptosis in Huh7 cells (Fig. 6B). A Western blot analysis revealed that silencing ZYX impeded the phosphorylation of FAK and AKT, whereas ITGB1 expression remained unaffected (Fig. 6C). Moreover, ZYX knockdown influenced the expression of apoptosis- and EMT-related proteins (Fig. 6D), inhibited EMT and induced apoptosis in Huh7 cells. These results indicate that ZYX operates downstream of ITGB1 and plays important roles in suppressing the in vitro progression of HCC cells.

ZYX interacts with ITGB1 to facilitate HCC development

We cotransfected si-ZYX and pcDNA-ITGB1 into Huh7 cells to explore the potential interaction between ZYX and ITGB1. Functionally, ZYX knockdown attenuated the promotion of HCC cell migration, invasion and adhesion by ITGB1 (Fig. 7A). For further related mechanistic research, Western blot analysis revealed that ITGB1 increased the expression of ZYX and the phosphorylation of FAK and AKT, which were reversed by ZYX knockdown (Fig. 7B). Moreover, overexpression of ITGB1 suppressed apoptosis and triggered EMT in Huh7 cells, which was counteracted by ZYX knockdown (Fig. 7C). Our coimmunoprecipitation data further confirmed that ZYX could indeed bind with ITGB1 (Fig. 7D). Immunofluorescence staining revealed the colocalization of ITGB1 and ZYX in Huh7 cells (Fig. 7E). Overall, these results indicate that ZYX may promote HCC progression

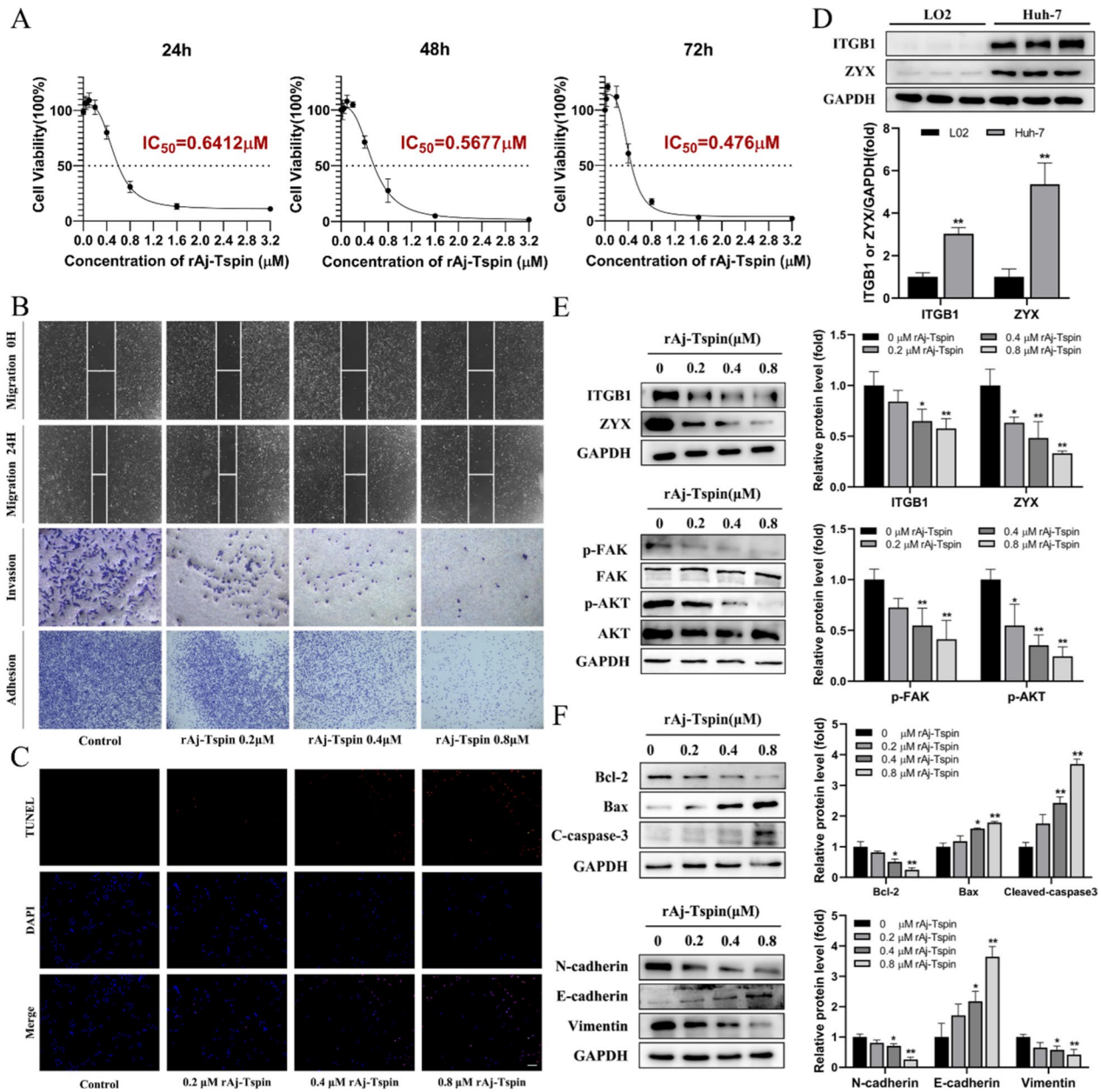

Fig. 3 rAj-Tspin inhibited the growth and promoted the apoptosis of Huh7 cells. **A** Measurement of cell viability upon rAj-Tspin treatment with a CCK-8 assay. **B** Migration, invasion and adhesion capacity of Huh7 cells treated with increasing concentrations (0, 0.2, 0.4, 0.8 μM) of rAj-Tspin for 24 h. **C** Apoptotic cells were examined via a TUNEL assay; scale bar = 50 μm. **D** Immunoblotting of ITGB1 and ZYX in LO2 and Huh7 cells. **E** and **F** Immunoblotting of ITGB1, ZYX, p-FAK, FAK, p-AKT, AKT, Bcl-2, Bax, cleaved caspase-3, vimentin, N-cadherin, and E-cadherin in Huh7 cells treated with increasing concentrations (0, 0.2, 0.4, 0.8 μM) of rAj-Tspin for 24 h (n = 3). $^{*}P < 0.05$, $^{**}P < 0.01$

by interacting with ITGB1 via the FAK/AKT signaling pathway.

Discussion

In this study, we demonstrated for the first time the inhibitory effect of rAj-Tspin on an orthotopic intrahepatic transplantation model, and we investigated the roles and mechanisms involved in the regulation of ITGB1/ZYX in response to rAj-Tspin treatment in HCC cells. Our data suggest that rAj-Tspin promotes apoptosis and inhibits EMT by suppressing the FAK/AKT pathway. We found that rAj-Tspin decreases ITGB1 and ZYX expression, contributing to HCC cell apoptosis and tumor suppression. To our knowledge, our findings reveal a novel

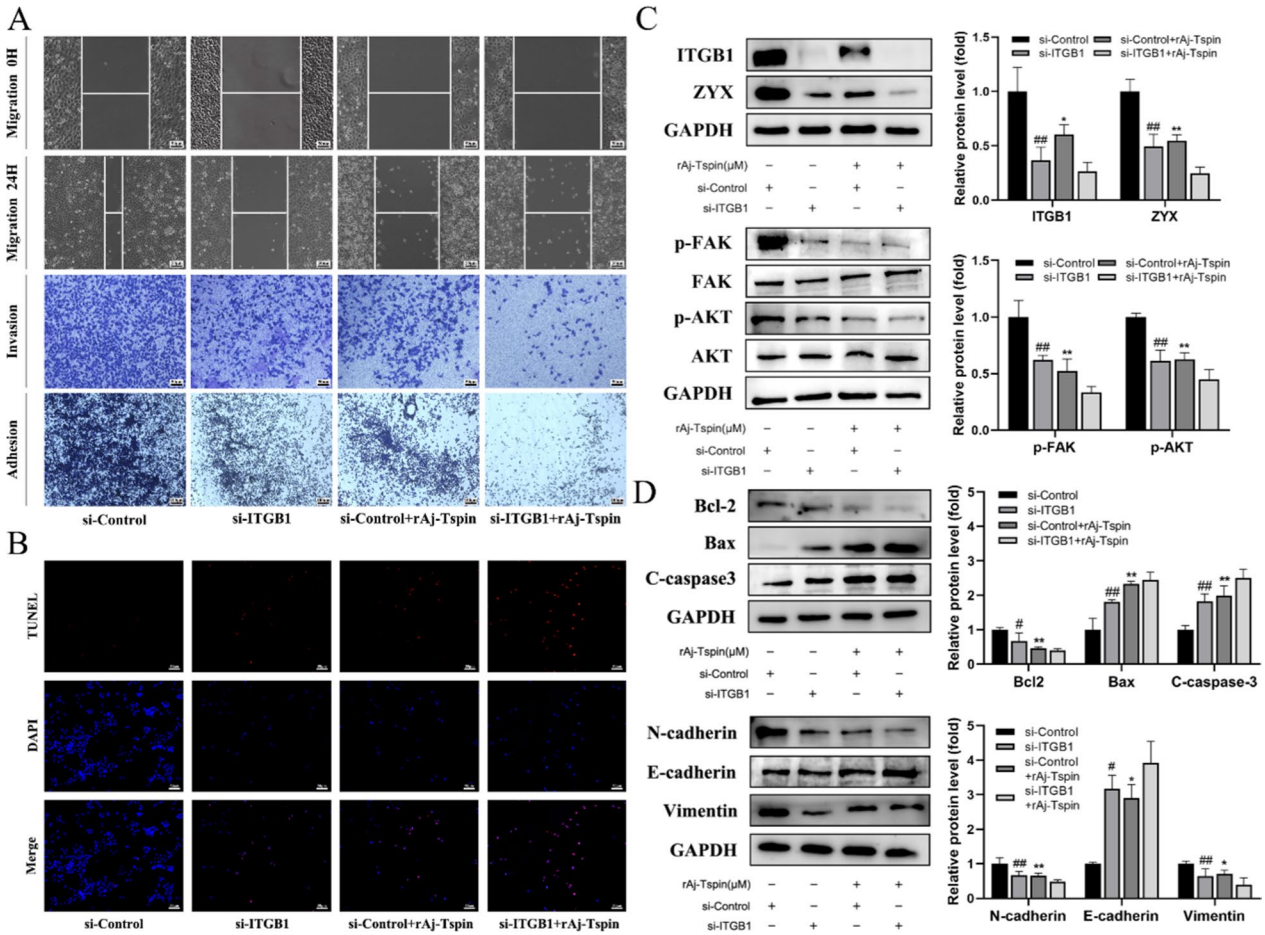

Fig. 4 ITGB1 knockdown inhibited growth and promoted apoptosis in Huh7 cells. ITGB1 was knocked down in Huh7 cells by siRNA treatment with or without 0.8 μM rAj-Tspin for 24 h. **A** Migration, invasion and adhesion capacity of Huh7 cells. **B** Apoptotic cells were examined via a TUNEL assay; scale bar = 50 μm. **C** and **D** Immunoblotting of ITGB1, ZYX, p-FAK, FAK, p-AKT, AKT, Bcl-2, Bax, cleaved caspase-3, vimentin, N-cadherin, and E-cadherin in Huh7 cells (n = 3). $^{\#}P < 0.05$, $^{\#\#}P < 0.01$, $^{*}P < 0.05$, $^{**}P < 0.01$

mechanism of rAj-Tspin-mediated HCC suppression, with a focus on the role of ITGB1 and ZYX in FAK/AKT pathway induction.

HCC is a prevalent and severe malignancy [22]. Radical hepatectomy remains the preferred therapeutic option for patients diagnosed with HCC in current clinical practice [23, 24]. However, the long-term prognosis remains unsatisfactory, with a high recurrence rate of 60% to 70% within five years postsurgery [25]. Therefore, the exploration of novel therapeutic drugs and targets is crucial for transforming the current state of medical treatment.

rAj-Tspin is a small polypeptide derived from *A. japonicus* that contains RGD modules. As a targeting ligand, RGD offers significant advantages in terms of targetability and safety [26]. Peptides containing the RGD domain have been demonstrated to exhibit specific recognition of integrin receptors, rendering them a precise therapeutic option for various tumors [27]. In the present study, our results indicated that rAj-Tspin can significantly inhibit the growth of axillary tumors and in situ tumors in nude mice.

HCC is a prevalent malignancy worldwide and is characterized by high recurrence rates and a poor prognosis due to the highly proliferative and invasive nature of HCC cells [28]. Loss of contact inhibition in cancer cells hinders apoptosis and promotes unlimited proliferation [29]. Various apoptosis markers, such as Bcl2, Bax and cleaved caspase-3, are associated with tumor progression. During the process of metastasis, individual tumor cells undergo EMT and subsequently invade the bloodstream [30]. EMT is characterized by the phenotypic transformation of cells from an epithelial to a mesenchymal state. Various epithelial and mesenchymal markers, such as vimentin, N-cadherin and E-cadherin, are associated with tumor progression. In our study, rAj-Tspin reduced proliferation by downregulating Bcl-2 and upregulating

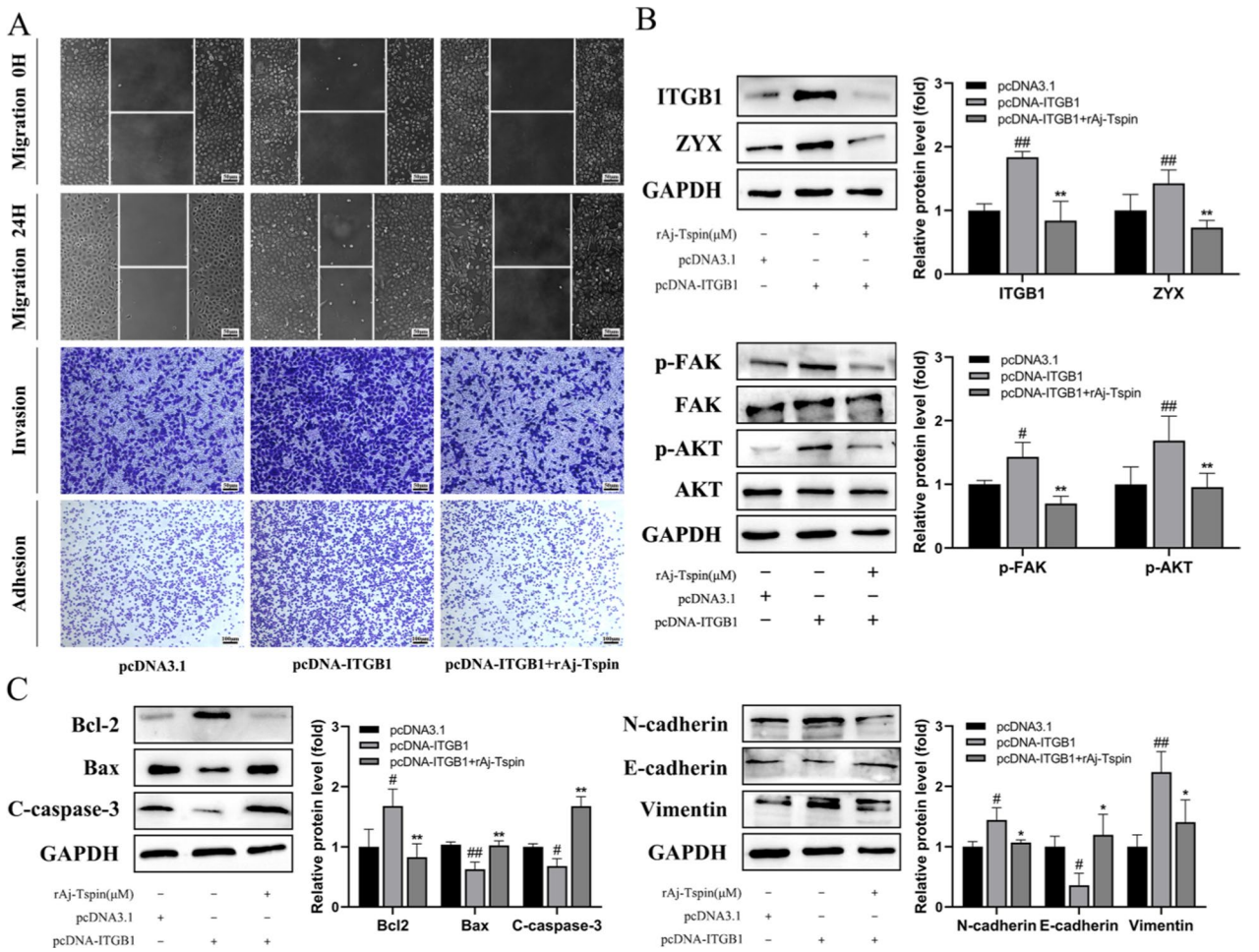

Fig. 5 rAj-Tspin suppressed HCC development via ITGB1. pcDNA3.1 or pcDNA-ITGB1 was transfected into Huh7 cells treated with or without 0.8 μM rAj-Tspin for 24 h. **A** Migration, invasion and adhesion capacity of Huh7 cells. **B** and **C** Immunoblotting of ITGB1, ZYX, p-FAK, FAK, p-AKT, AKT, Bcl-2, Bax, cleaved caspase-3, vimentin, N-cadherin, and E-cadherin in Huh7 cells (n = 3). $^{\#}P < 0.05$, $^{\#\#}P < 0.01$, $^{*}P < 0.05$, $^{**}P < 0.01$

Bax and cleaved caspase-3 and suppressed invasion by downregulating N-cadherin and vimentin and upregulating E-cadherin in HCC cells.

Integrin-mediated signal transduction has been shown to induce cytoskeletal rearrangement through focal adhesion, thereby promoting tumor cell proliferation, invasion, and metastasis in cancer [31]. The extracellular domain of integrin interacts with ligands in the ECM, subsequently triggering downstream signaling pathways, which typically involve a series of phosphorylation events, such as FAK and AKT [32, 33]. Compared with the expression of other integrin subtypes, the expression of ITGB1 is significantly greater in liver tumor tissues. Multiple studies have demonstrated that ITGB1 inhibition markedly inhibits the growth of HCC cells via apoptosis induction and EMT inhibition [34, 35]. Our previous study revealed that rAj-Tspin is able to inhibit the development of HCC by inhibiting the FAK/AKT and ITGB1 signaling pathways [13]. However, the detailed functions of ITGB1 in the pathogenesis of HCC have not been completely elucidated. Our current study revealed that rAj-Tspin treatment decreases ITGB1 expression in a dose-dependent manner both in vivo and in vitro and that the overexpression of ITGB1 can be inhibited by rAj-Tspin, suggesting that rAj-Tspin is a potential ITGB1 inhibitor. Moreover, manipulation of ITGB1 expression levels through knockdown or overexpression can modulate the FAK/AKT signaling pathway, EMT progression, and cellular apoptosis.

Generally, adhesion between cells and the extracellular matrix is a crucial factor for cancer cells [27]. Focal adhesion has been identified as the pivotal determinant among the various microenvironmental factors that influence drug resistance in cancer cells [36]. ZYX is a pivotal protein associated with EMT and apoptosis in focal adhesions. High expression of ZYX in cancer is

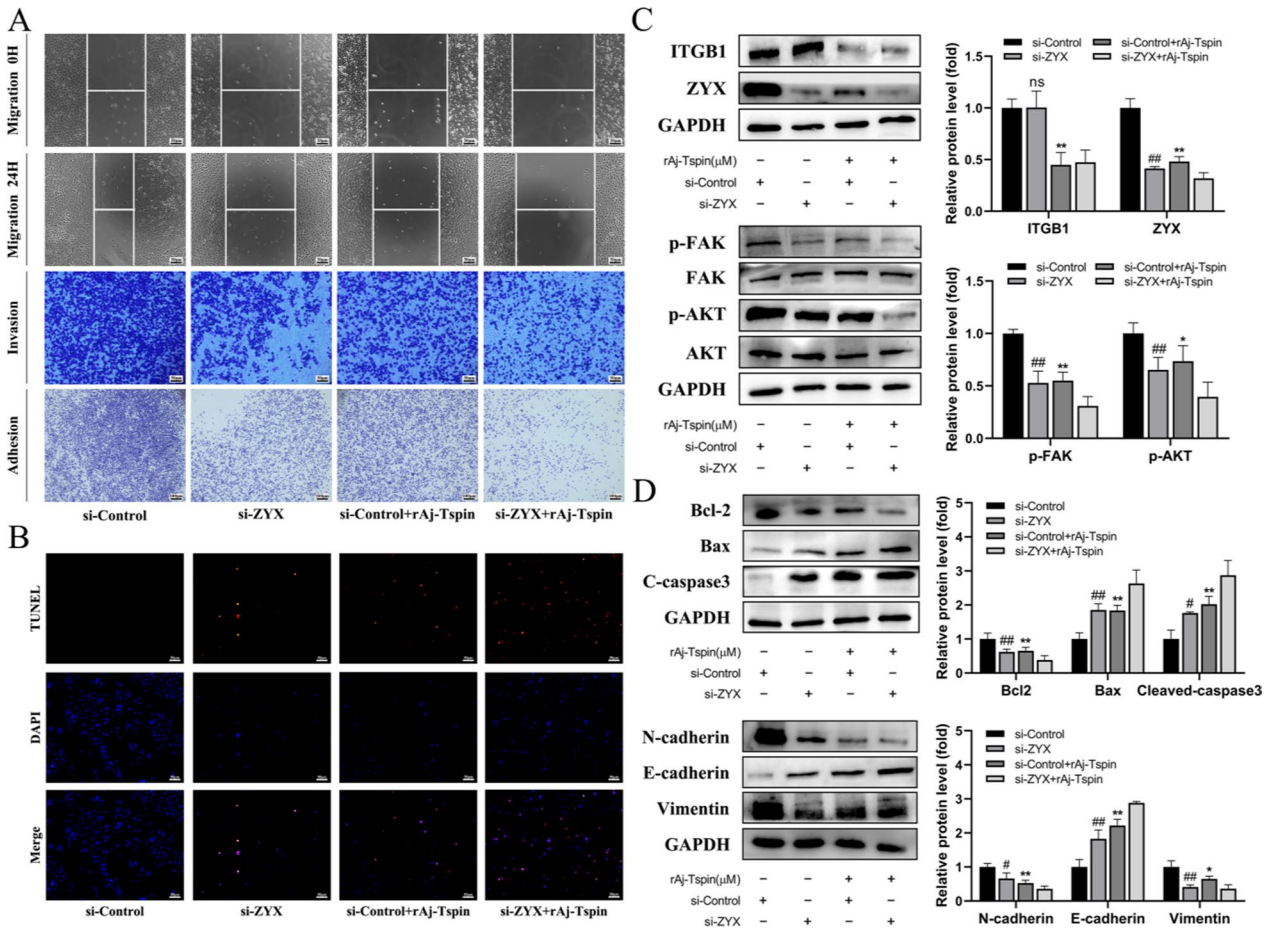

Fig. 6 ZYX knockdown inhibited growth and promoted apoptosis in Huh7 cells. ZYX was knocked down in Huh7 cells by siRNA treated with or without 0.8 μM rAj-Tspin for 24 h. **A** Migration, invasion and adhesion capacity of Huh7 cells. **B** Apoptotic cells were examined via a TUNEL assay; scale bar = 50 μm. **C** and **D** Immunoblotting of ITGB1, ZYX, p-FAK, FAK, p-AKT, AKT, Bcl-2, Bax, cleaved caspase-3, vimentin, N-cadherin, and E-cadherin in Huh7 cells (n = 3). $^{ns}P > 0.05$, $^{\#}P < 0.05$, $^{\#\#}P < 0.01$, $^{*}P < 0.05$, $^{**}P < 0.01$

closely correlated with more aggressive behavior, a lower apoptotic ratio and diminished overall survival [37]. First, ZYX was overexpressed in both HCC tissues and cell lines, and the administration of rAj-Tspin led to a dose-dependent reduction in ZYX expression both in vivo and in vitro. After ZYX was knocked down with a specific interfering RNA, we discovered that ZYX mediated the proliferation and metastasis of HCC cells in vitro. These results indicated that ZYX might act as an oncogene in HCC progression. Moreover, co-IP and immunofluorescence assays demonstrated the interaction and colocalization of ZYX with ITGB1. Our in-depth research also revealed that ITGB1 promoted the activation of the FAK/AKT pathway, which was mediated by ZYX.

Taken together, the results of this study provide compelling evidence that ZYX is involved in the effects of rAj-Tspin treatment on HCC and that ITGB1 downregulation plays an inhibitory role in the FAK/AKT pathway by suppressing ZYX expression, resulting in cell death and tumor suppression. These findings offer innovative insights into the mechanism of action of rAj-Tspin, suggesting that rAj-Tspin is a potential therapeutic agent against HCC and highlighting the ITGB1/ZYX/FAK/AKT axis as a promising target for cancer treatment.

The present study enhances the comprehensive understanding of HCC pathogenesis, offers novel targets and medications for targeted therapy of HCC, and provides fresh insights into the treatment of this malignancy. However, the range of samples utilized for experimental verification in this research is limited, and the current experiment has only been validated at the cellular and murine levels. The lack of corresponding clinical samples restricts the applicability of the drug in a clinical setting. Potential future endeavors encompass conducting clinical response experiments and expanding investigations into cancer indications for this medication. The

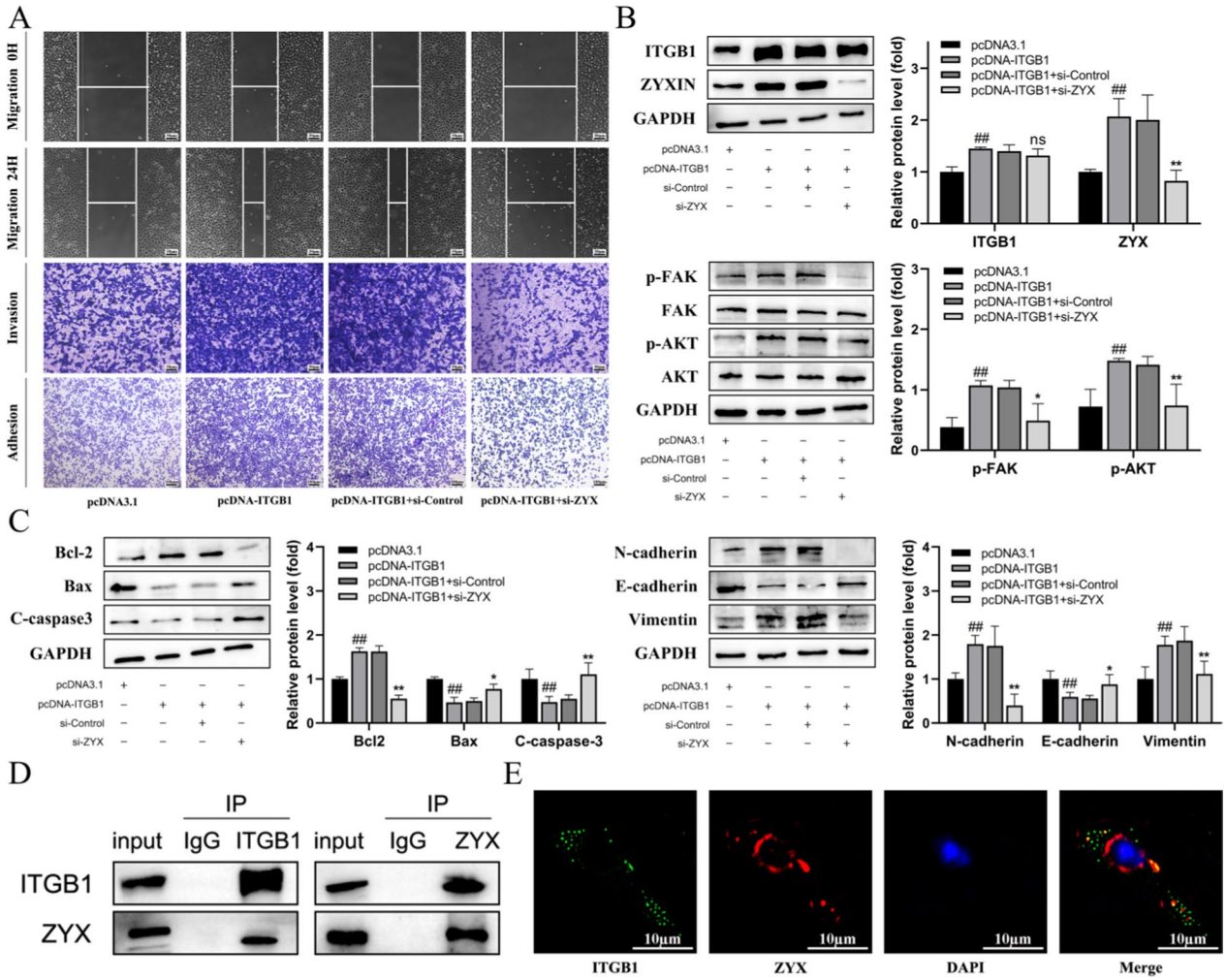

Fig. 7 The ITGB1/ZYX axis was validated in Huh7 cells. pcDNA3.1 or pcDNA-ITGB1 was transfected into Huh7 cells with or without ZYX knockdown by siRNA for 24 h. **A** Migration, invasion and adhesion capacity of Huh7 cells. **B** and **C** Immunoblotting of ITGB1, ZYX, p-FAK, FAK, p-AKT, AKT, Bcl-2, Bax, cleaved caspase-3, vimentin, N-cadherin, and E-cadherin in Huh7 cells (n = 3). **D** Coimmunoprecipitation (Co-IP) assays were conducted in Huh7 cells transfected with a vector containing flag-tagged ITGB1 and ZYX; IgG was used as a control. **E** Confocal microscopy of immunofluorescence staining revealed that ITGB1 (green) colocalized with ZYX (red) in Huh7 cells. DAPI was used for nuclear staining; scale bar = 10 μm. $^{\#}P < 0.05$, $^{\#\#}P < 0.01$, $^{*}P < 0.05$, $^{**}P < 0.01$

prognosis of HCC is generally unfavorable, and the prevention and control of this disease remain a formidable challenge, characterized by a low 5-year survival rate. Researchers should possess a comprehensive knowledge system and professional expertise to gain profound insights into the evolutionary mechanism of HCC and employ multidisciplinary collaboration to determine the most suitable treatment plan. In the next 5 years, there will be continuous innovations in HCC treatment research, with close integration of clinical and basic research. The rapid translation of research findings into clinical practice aims to increase the survival benefits for patients with HCC.

Abbreviations

AKT	Protein kinase B
BCA	Bicinchoninic acid
DMEM	Dulbecco's modified Eagle's medium
EMT	Epithelial–mesenchymal transition
FAK	Focal adhesion kinase
FBS	Fetal bovine serum
H&E	Hematoxylin and eosin
HCC	Hepatocellular carcinoma
ITGB1	Integrin β1
PBS	Phosphate-buffered saline
PVDF	Polyvinylidene difluoride
RGD	Arginine–glycine–aspartic acid
rAj-Tspin	Recombinant *Apostichopus japonicus* rAj-Tspin polypeptide
SDS-PAGE	Sodium dodecyl sulfate-polyacrylamide gel electrophoresis
ZYX	Zyxin

Acknowledgements
Not applicable.

Author contributions
YC, XTW, JHW, ZCZ and LL designed the experiments. YC wrote the manuscript. YC, XTW, LYG, XL, ZXD, ZEL and HR performed the animal experiments. YC performed the Western blot assays. YC, XLL and LL edited the manuscript. YC generated the statistical analysis and handled the figure data.

Funding
This work was supported by the Liaoning Provincial Department of Education Service Local Project (grant number LJKFZ20220251).

Availability of data and materials
No datasets were generated or analysed during the current study.

Declarations

Ethics approval and consent to participate
The experiments related to laboratory animal testing involved in the 2020 National Natural Science Foundation of China project "Antitumor function of the recombinant peptide rAj-Tspin mimicking spiny ginseng and its mechanism of action", were examined by the Ethics Committee of Liaoning Normal University, which concluded that the project complied with the requirements of ethics and agreed with the filing.

Consent for publication
Not applicable.

Competing interests
The authors declare no competing interests.

Author details
[1]Department of Pharmacology, Dalian Medical University, Dalian 116044, Liaoning, China. [2]Liaoning Ocean and Fisheries Science Research Institute, Dalian 116023, Liaoning, China. [3]School of Life Sciences, Liaoning Normal University, Dalian 116081, Liaoning, China.

Received: 9 August 2023 Accepted: 29 July 2024
Published online: 14 August 2024

References

1. Vogel A, Meyer T, Sapisochin G, Salem R, Saborowski A. Hepatocellular carcinoma. Lancet. 2022;400(10360):1345–62.
2. Lee TK-W, Guan X-Y, Ma S. Cancer stem cells in hepatocellular carcinoma - from origin to clinical implications. Nat Rev Gastroenterol Hepatol. 2022;19(1):26–44.
3. Sankar K, Gong J, Osipov A, Miles SA, Kosari K, Nissen NN, Hendifar AE, Koltsova EK, Yang JD. Recent advances in the management of hepatocellular carcinoma. Clin Mol Hepatol. 2024;30(1):1–15.
4. Rizzo A, Ricci AD, Brandi G. Trans-arterial chemoembolization plus systemic treatments for hepatocellular carcinoma: an update. J Pers Med. 2022;12(11):1788.
5. Bent EH, Wehrenberg-Klee E, Koay EJ, Goyal L, Wo JY. Integration of systemic and liver-directed therapies for locally advanced hepatocellular cancer: harnessing potential synergy for new therapeutic horizons. J Natl Compr Canc Netw. 2021;19(5):567–76.
6. Rizzo A, Ricci AD, Brandi G. Atezolizumab in advanced hepatocellular carcinoma: good things come to those who wait. Immunotherapy. 2021;13(8):637–44.
7. Shen K-Y, Zhu Y, Xie S-Z, Qin L-X. Immunosuppressive tumor microenvironment and immunotherapy of hepatocellular carcinoma: current status and prospectives. J Hematol Oncol. 2024;17(1):25.
8. Pinter M, Scheiner B, Peck-Radosavljevic M. Immunotherapy for advanced hepatocellular carcinoma: a focus on special subgroups. Gut. 2021;70(1):204–14.
9. Lv Z, Yue Z, Shao Y, Li C, Zhao X, Guo M. mTORC2/Rictor is essential for coelomocyte endocytosis in *Apostichopus japonicus*. Dev Comp Immunol. 2021;118: 104000.
10. Qiao R, Xiao R, Chen Z, Jiang J, Yuan C, Ning S, Wang J, Zhou Z. Cloning, expression and inhibitory effects on lewis lung carcinoma cells of rAj-Tspin from sea cucumber (*Apostichopus japonicus*). Molecules (Basel Switzerland). 2021;27(1):229.
11. Casal JI, Bartolomé RA. RGD cadherins and α2β1 integrin in cancer metastasis: a dangerous liaison. Biochim Biophys Acta Rev Cancer. 2018;1869(2):321–32.
12. Sheikh A, Md S, Kesharwani P. RGD engineered dendrimer nanotherapeutic as an emerging targeted approach in cancer therapy. J Control Release. 2021;340:221–42.
13. Yu P, Wu R, Zhou Z, Zhang X, Wang R, Wang X, Lin S, Wang J, Lv L. rAj-Tspin, a novel recombinant peptide from *Apostichopus japonicus*, suppresses the proliferation, migration, and invasion of BEL-7402 cells via a mechanism associated with the ITGB1-FAK-AKT pathway. Invest New Drugs. 2021;39(2):377–85.
14. He M, Zhou Z, Wu G, Chen Q, Wan Y. Emerging role of DUBs in tumor metastasis and apoptosis: therapeutic implication. Pharmacol Ther. 2017;177:96–107.
15. Zhong C, Yu J, Li D, Jiang K, Tang Y, Yang M, Shen H, Fang X, Ding K, Zheng S, Yuan Y. Zyxin as a potential cancer prognostic marker promotes the proliferation and metastasis of colorectal cancer cells. J Cell Physiol. 2019;234:15775–89.
16. Partynska A, Gomulkiewicz A, Piotrowska A, Grzegrzolka J, Rzechonek A, Ratajczak-Wielgomas K, Podhorska-Okolow M, Dziegiel P. Expression of zyxin in non-small cell lung cancer-a preliminary study. Biomolecules. 2022;12(6):827.
17. Wen X-M, Luo T, Jiang Y, Wang L-H, Luo Y, Chen Q, Yang K, Yuan Y, Luo C, Zhang X, Yan Z-X, Fu W-J, Tan Y-H, Niu Q, Xiao J-F, Chen L, Wang J, Huang J-F, Cui Y-H, Zhang X, Wang Y, Bian X-W. Zyxin (ZYX) promotes invasion and acts as a biomarker for aggressive phenotypes of human glioblastoma multiforme. Lab Invest. 2020;100(6):812–23.
18. Paluch EK, Aspalter IM, Sixt M. Focal adhesion-independent cell migration. Annu Rev Cell Dev Biol. 2016;32:469–90.
19. Seong J, Wang N, Wang Y. Mechanotransduction at focal adhesions: from physiology to cancer development. J Cell Mol Med. 2013;17(5):597–604.
20. Li Z-J, Dai H-Q, Huang X-W, Feng J, Deng J-H, Wang Z-X, Yang X-M, Liu Y-J, Wu Y, Chen P-H, Shi H, Wang J-G, Zhou J, Lu G-D. Artesunate synergizes with sorafenib to induce ferroptosis in hepatocellular carcinoma. Acta Pharmacol Sin. 2021;42(2):301–10.
21. El-Shemi AG, Ashshi AM, Na Y, Li Y, Basalamah M, Al-Allaf FA, Oh E, Jung B-K, Yun C-O. Combined therapy with oncolytic adenoviruses encoding TRAIL and IL-12 genes markedly suppressed human hepatocellular carcinoma both in vitro and in an orthotopic transplanted mouse model. J Exp Clin Cancer Res. 2016;35:74.
22. Xu X-F, Xing H, Han J, Li Z-L, Lau W-Y, Zhou Y-H, Gu W-M, Wang H, Chen T-H, Zeng Y-Y, Li C, Wu M-C, Shen F, Yang T. Risk factors, patterns, and outcomes of late recurrence after liver resection for hepatocellular carcinoma: a multicenter study from China. JAMA Surg. 2019;154(3):209–17.
23. Chidambaranathan-Reghupaty S, Fisher PB, Sarkar D. Hepatocellular carcinoma (HCC): Epidemiology, etiology and molecular classification. Adv Cancer Res. 2021;149:1–61.
24. Chen Y, Chen H-N, Wang K, Zhang L, Huang Z, Liu J, Zhang Z, Luo M, Lei Y, Peng Y, Zhou Z-G, Wei Y, Huang C. Ketoconazole exacerbates mitophagy to induce apoptosis by downregulating cyclooxygenase-2 in hepatocellular carcinoma. J Hepatol. 2019;70(1):66–77.
25. Liu D, Song T. Changes in and challenges regarding the surgical treatment of hepatocellular carcinoma in China. Biosci Trends. 2021;15(3):142–7.
26. Li T, Zhou T, Liu Y, Wang J, Yu Z. Efficacy analysis of targeted nanodrug for non-small cell lung cancer therapy. Front Bioeng Biotechnol. 2022;10:1068699.
27. Fu S, Xu X, Ma Y, Zhang S, Zhang S. RGD peptide-based non-viral gene delivery vectors targeting integrin αvβ3 for cancer therapy. J Drug Target. 2019;27:1–11.

28. Yang JD, Hainaut P, Gores GJ, Amadou A, Plymoth A, Roberts LR. A global view of hepatocellular carcinoma: trends, risk, prevention and management. Nat Rev Gastroenterol Hepatol. 2019;16(10):589–604.
29. Eke I, Cordes N. Focal adhesion signaling and therapy resistance in cancer. Semin Cancer Biol. 2015;31:65–75.
30. Liao S, Chen H, Liu M, Gan L, Li C, Zhang W, Lv L, Mei Z. Aquaporin 9 inhibits growth and metastasis of hepatocellular carcinoma cells via Wnt/β-catenin pathway. Aging (Albany NY). 2020;12(2):1527–44.
31. Mygind KJ, Schwarz J, Sahgal P, Ivaska J, Kveiborg M. Loss of ADAM9 expression impairs β1 integrin endocytosis, focal adhesion formation and cancer cell migration. J Cell Sci. 2018;131(1):jcs205393.
32. Shang N, Arteaga M, Zaidi A, Stauffer J, Cotler SJ, Zeleznik-Le NJ, Zhang J, Qiu W. FAK is required for c-Met/β-catenin-driven hepatocarcinogenesis. Hepatology. 2015;61(1):214–26.
33. Ma H, Wang J, Zhao X, Wu T, Huang Z, Chen D, Liu Y, Ouyang G. Periostin promotes colorectal tumorigenesis through integrin-FAK-Src pathway-mediated YAP/TAZ activation. Cell Rep. 2020;30(3):793–806.
34. Guo D, Zhang D, Ren M, Lu G, Zhang X, He S, Li Y. THBS4 promotes HCC progression by regulating ITGB1 via FAK/PI3K/AKT pathway. FASEB J. 2020;34(8):10668–81.
35. Sun Q, Zhou C, Ma R, Guo Q, Huang H, Hao J, Liu H, Shi R, Liu B. Prognostic value of increased integrin-beta 1 expression in solid cancers: a meta-analysis. Onco Targets Ther. 2018;11:1787–99.
36. Liu M, Yan R, Wang J, Yao Z, Fan X, Zhou K. LAPTM4B-35 promotes cancer cell migration via stimulating integrin beta1 recycling and focal adhesion dynamics. Cancer Sci. 2022;113(6):2022–33.
37. Yamamura M, Noguchi K, Nakano Y, Segawa E, Zushi Y, Takaoka K, Kishimoto H, Hashimoto-Tamaoki T, Urade M. Functional analysis of Zyxin in cell migration and invasive potential of oral squamous cell carcinoma cells. Int J Oncol. 2013;42(3):873–80.

Publisher's Note